Intramolecular Charge Transfer of Push–Pull Pyridinium Salts in the Triplet Manifold

ARTICLE *in* THE JOURNAL OF PHYSICAL CHEMISTRY A · APRIL 2014

Impact Factor: 2.69 · DOI: 10.1021/jp407342q · Source: PubMed

6 AUTHORS, INCLUDING:

Benedetta Carlotti
Università degli Studi di Perugia
40 PUBLICATIONS **296** CITATIONS
SEE PROFILE

Giuseppe A. Consiglio
University of Catania
54 PUBLICATIONS **550** CITATIONS
SEE PROFILE

Fausto Elisei
Università degli Studi di Perugia
193 PUBLICATIONS **3,403** CITATIONS
SEE PROFILE

Anna Spalletti
Università degli Studi di Perugia
102 PUBLICATIONS **1,203** CITATIONS
SEE PROFILE

THE JOURNAL OF PHYSICAL CHEMISTRY A

Article

pubs.acs.org/JPCA

Intramolecular Charge Transfer of Push−Pull Pyridinium Salts in the Singlet Manifold

Benedetta Carlotti,[†] Giuseppe Consiglio,[‡] Fausto Elisei,[†] Cosimo G. Fortuna,[‡] Ugo Mazzucato,[†] and Anna Spalletti*[,†]

[†]Department of Chemistry, Biology and Biotechnology and Centro di Eccellenza sui Materiali Innovativi Nanostrutturati (CEMIN), University of Perugia, via Elce di Sotto 8, 06123 Perugia, Italy

[‡]Department of Chemical Sciences, University of Catania, viale Andrea Doria 6, 95125 Catania, Italy

Supporting Information

ABSTRACT: The solvent effect on the photophysical and photochemical properties of the iodides of three *trans* (*E*) isomers of 2-D-vinyl,1-methylpyridinium, where D is a donor group (4-dimethylaminophenyl, 3,4,5-trimethoxyphenyl and 1-pyrenyl), was studied by stationary and transient absorption techniques. The results obtained allowed the negative solvatochromism and relaxation pathways of the excited states in the singlet manifold to be reasonably interpreted. Resorting to ultrafast absorption techniques and DFT calculations allowed information on the excited state dynamics and the role of the solvent-controlled intramolecular charge transfer (ICT) processes to be obtained. The structure-dependent excited state dynamics in nonpolar solvents, where the ICT is slower than solvent rearrangement, and in polar solvents, where an opposite situation is operative, was thus explained. The push−pull character of the three compounds, particularly the anilino-derivative, suggests their potential application in optoelectronics.

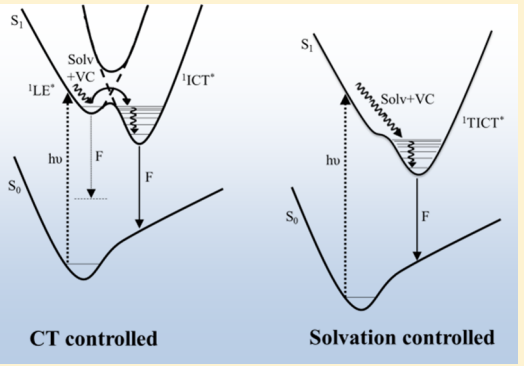

1. INTRODUCTION

In the framework of our long-term project on the internal rotation around double and single bonds, we have recently been concerned with the study of quaternized azastilbenes[1−4] since methyl-pyridinium salts and analogous compounds could be of interest for potential applications in the medical fields, due to their ability to form complexes with DNA,[5,6] and in optoelectronics/photonics as nonlinear optical (NLO) materials.[7] In particular, dimethylamino-derivatives have also been used as fluorescent sensors[8] since the introduction of the anilino group can affect significantly the quantum yields of the competitive reactive (trans → cis photoisomerization) and radiative deactivation.[9]

Solvent polarity is expected to substantially influence the photobehavior of these ionic dipolar compounds where electron-donor groups and electron deficient pyridinium units are present. The positive solvatochromism of push−pull systems is well documented[10−14] whereas the negative solvatochromism, where the molecular dipole moment is expected to decrease under excitation, has been less studied.[8,9,12,15] In this paper the effect of solvent polarity on the spectral and photophysical properties of two stilbazolium salts and a pyrenyl-analogue, namely the iodides of the *trans* (*E*) isomers of the 2-D-vinyl,1-methylpyridinium cations where D is a donor group [4-dimethylaminophenyl, (**1**), 3,4,5-trimethoxyphenyl (**2**) and 1-pyrenyl (**3**)] (Scheme 1), were investigated by stationary and transient absorption techniques and DFT calculations. The photobehavior of the polar **1** (usually named by its acronym *o*-DASPMI) and its positional isomer *p*-DASPMI, were previously studied in various laboratories by stationary and ultrafast spectroscopic techniques.[9,16−30] For **1**, a negative solvatochromism and a very modest, if any, positive fluosolvatochromism were reported. The solvent-dependent excited state dynamics, which involves internal rotation around double (cis−trans isomerization) and single (formation of twisted rotamers) bonds, was discussed using different approaches. Some authors mainly emphasized the effects of solvent dynamics reflected by the fastest decay components[25,26,28,29] while others gave more attention to the concomitant evolution of the excited solute on the basis of a three-state model.[23,24,27] These authors attributed the multiexponential emission specifically to the contributions of the locally excited (LE) state, formed by the relaxation of the Franck−Condon state and precursor of a second state (still planar), produced by further intramolecular charge transfer (ICT), generally favored in polar solvents, and a successive third state formed in polar solvents by the twisting of the *p*-dimethylanilino or *N*-methylpyridinium group around the quasi-single bond with the ethene bridge (TICT).[23,24,27] As pointed out in previous papers[23,29] both aspects, the relaxation

Received: July 24, 2013
Revised: April 29, 2014

   dx.doi.org/10.1021/jp407342q | J. Phys. Chem. A XXXX, XXX, XXX−XXX

Scheme 1. Molecular Structures of the Trans (*E*) Cations of the Iodides of 2-D-Ethenyl-1-methylpyridinium (D = 4-(Dimethylamino)phenyl (1), 3,4,5-Trimethoxyphenyl (2), and 1-Pyrenyl (3)

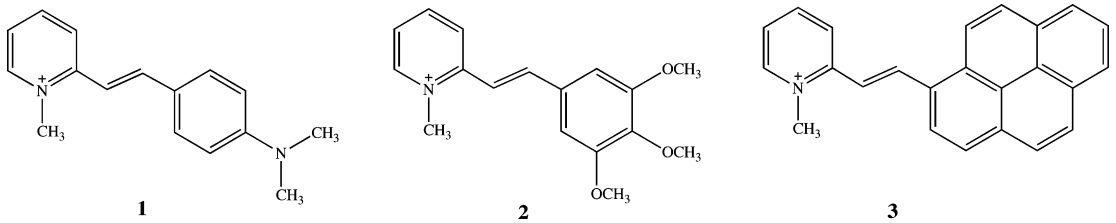

of solvent dipoles and the detection of several emitting states, have to be taken into account when describing the emission properties of these kind of dyes.

The main aim of the present work is 2-fold. Using ultrafast techniques and with the help of DFT calculations we obtain information on the excited state behavior of **1** in the singlet manifold and in a wide series of solvents of different polarity thus allowing the solvent-controlled ICT process and its dynamics to be exhaustively interpreted. Moreover, we extend the measurements to the new **2** and **3** analogues, to compare the behavior of the three compounds having electron donor properties of different efficiency, in order to better understand the role of the ICT process in these molecules and the competition between the solvent organization and the charge movement in the solutes. Contrary to what generally reported in the literature, the new results indicate that the relaxed ICT state (or TICT, in the case of compounds **1** and **2**) reflects a back localization of the positive charge on the pyridinium group.

2. EXPERIMENTAL SECTION

2.1. Materials. The investigated compounds **1**−**3** are shown in Scheme 1. They were synthesized as iodide salts at the Catania Laboratory following the procedure described in previous works.[5,6]

Measurements were performed in various organic solvents of different polarity: chloroform ($CHCl_3$), dichloromethane (DCM), 1,2-dichloroethane (DCE), acetone (Ac), acetonitrile (MeCN), dimethyl sulfoxide (DMSO), ethanol (EtOH), methanol (MeOH), 2-propanol (2-PrOH), water (W), and glycerol (Gly). All solvents were from Fluka (spectrophotometric grade) and were used without further purification.

2.2. Photophysical and Photochemical Measurements. A PerkinElmer Lambda 800 spectrophotometer was used for absorption measurements. The fluorescence spectra were measured by a Spex Fluorolog-2 F112AI spectrofluorimeter. Dilute solutions (absorbance <0.1 at the excitation wavelength, λ_{exc}) were used for fluorimetric measurements. The fluorescence quantum yield (ϕ_F, uncertainty ±10%) was determined at λ_{exc} corresponding to the maximum of the first absorption band (λ_{max}). Tetracene (ϕ_F = 0.17[31] in aerated CH) and 9,10-diphenylanthracene (ϕ_F = 0.90,[32] in deaerated CH) were used as fluorimetric standards.

A detailed description of the experimental setup for ultrafast spectroscopic and kinetic measurements was previously reported.[33,34] The 400 nm excitation pulses of ca. 60 fs were generated by an amplified Ti:sapphire laser system (Spectra Physics, Mountain View, CA). The transient absorption set up (Helios, Ultrafast Systems) is characterized by temporal resolution of ca. 150 fs and spectral resolution of 1.5 nm. All measurements were carried out under magic angle in a 2 mm cell at an absorbance of about 0.5 at 400 nm. The solution was stirred during the experiments to avoid photoproduct interferences. Transient absorption data were analyzed using the Surface Xplorer PRO (Ultrafast Systems) software where it was possible to perform singular value decomposition[35,36] of the 3D surface into the principal components (spectra and kinetics) and to perform global analysis (giving lifetimes and decay associated spectra (DAS) of the detected transients)[37] with a number of components determined on the basis of best fitting procedure. Target analysis assuming several successive steps and resulting in the species associated spectra (SAS) was also used to globally fit the acquired data by using Glotaran.[38] Only consecutive first order reactions were considered.

For photochemical measurements, a xenon lamp coupled with an interferential filter (λ_{exc} = 436 or 325 nm) and potassium ferrioxalate in 0.1 N sulfuric acid as actinometer were used. The photoreaction (solute concentration ~10^{-4} M) was monitored by HPLC using a Waters apparatus equipped with a Phenomenex Jupiter C18−300 Å (4.6 × 250 mm; 5 μm) column and an UV detector. W/MeCN mixtures with some addition of trifluoroacetic acid were used as eluent. The monitoring wavelength was at the isosbestic point between trans and cis absorption spectra, detected by irradiating the trans isomer in the eluent mixture. The conversion percentage was held below 10% to avoid the competition from the back photoreaction and the experimental error on the photoisomerization quantum yield is about ±10%. All measurements were performed at room temperature.

2.3. Theoretical Calculations. Simple theoretical calculations of the electronic spectra, conformational equilibria and heats of formation of the cations were carried out using the HyperChem computational package (version 7.5). The computed transition energies and oscillator strengths were obtained by ZINDO/S using optimized geometries (according to PM3 method) including 400 (20 × 20) single excited configurations.

Mulliken charges and dipole moments in the ground and excited singlet state (both in the vertical and relaxed conformation) were obtained by quantum-mechanical calculations using Gaussian 09 package[39] by taking also into account the solvent effect in the ground and excited states through the conductor polarizable continuum model (CPMC).[40] Density functional theory (DFT) B3LYP/3-21G* was used to optimize the ground state geometry of the substrates while the lowest excited singlet states were characterized by time dependent DFT excited-state calculations (TD-DFT/B3LYP/3-21G*). Dipole moments were obtained by the Mulliken atomic charges.[41,42]

As generally applied to these kinds of salts,[43,44] the calculations refer to the monochromophoric cations. To confirm the validity of this assumption we also did some calculations using the B3LYP/3.21G method on the reference

dx.doi.org/10.1021/jp407342q | J. Phys. Chem. A XXXX, XXX, XXX−XXX

compound **1** that allowed the counterion to be considered (see section 3 in the Supporting Information).

3. RESULTS AND DISCUSSION

3.1. Spectral Properties and Solvatochromism. The absorption and emission spectra of **1**−**3** were measured in a large series of solvents as a function of the E_T^N parameter, based on the pyridinium *N*-phenolate betaine.[45]

The salts were considered completely dissolved as free ions surrounded by solvent without any clear evidence of ion-pair formation. In a detailed study on the para-isomer of compound **1**, the presence of ion-pair was evidenced in solvents of $E_T^N < 0.3$.[46] On the basis of this result, some contribution of ion pairs could be expected in $CHCl_3$ only ($E_T^N = 0.259$). In fact, some anomalies found in the behavior of **1**−**3** in $CHCl_3$, such as the blue shift of the absorption maximum with respect to DCM or a too low ϕ_F (see below), could be related to partial contribution of ion-pairs.

Generally the spectra show nonstructured, intense and bell-shaped bands (Figure 1 shows an example in DCE). The

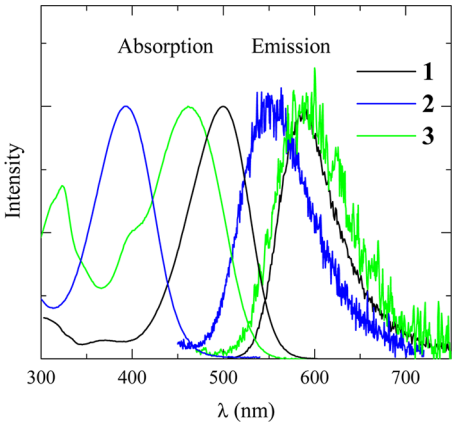

Figure 1. Normalized absorption and emission spectra of the investigated compounds in DCE.

spectral behavior of **1** in a few solvents was already reported in previous papers[16−20,22−29] but was here revisited to extend the range of solvents examined (see section 3.5 on the ultrafast measurements) and to compare the results for the three compounds under the same experimental conditions. The absorption spectra of **1** shift notably toward the blue on increasing the solvent polarity (Table 1 and Figure 2) in agreement with literature results.[16−20,22−29] On passing from a nonpolar and nonprotic DCM to the polar and protic W, a significant blue shift of about 60 nm was observed. It should be noted that hydrogen-bonding solvents, hampering the displacement of charge, can also contribute to the blue shift of the absorption spectrum. This could offer another explanation as to why the λ_{abs}^{max} values in $CHCl_3$ do not fit the trend as a function of the E_T^N parameter.[17,21]

In contrast to the absorption trend, the weak emission, centered at ∼600 nm, is influenced very little by the solvent. This behavior can be considered normal for ionic systems having a large dipole moment in the ground state that decreases under excitation, as found by the quantum-mechanical calculations (see below).

The behavior of our ionic compounds is in a net contrast to the better known corresponding neutral [4-(dimethylamino)-styryl]pyridines[47−49] where the dipole moment increases under

Table 1. Spectral Properties of 1 in Solvents of Increasing E_T^N Parameters

solvent	E_T^N	λ_{abs}/nm	λ_{em}/nm	$\Delta\nu$/cm^{-1}
$CHCl_3$	0.259	484	577	3330
DCM	0.309	500	590	3090
DCE	0.327	497	594	3285
Ac	0.355	458	603	5250
DMSO	0.441	460	610	5350
MeCN	0.472	456	600	5260
2-PrOH	0.546	469	583	4170
EtOH	0.654	467	589	4435
MeOH	0.762	462	590	4695
MeOH/Gly (50/50)	0.787	464	588	4545
W/EtOH (50/50)	0.827	460	585	4645
W/EtOH (70/30)	0.896	451	585	5080
W	1.0	438	589	5850

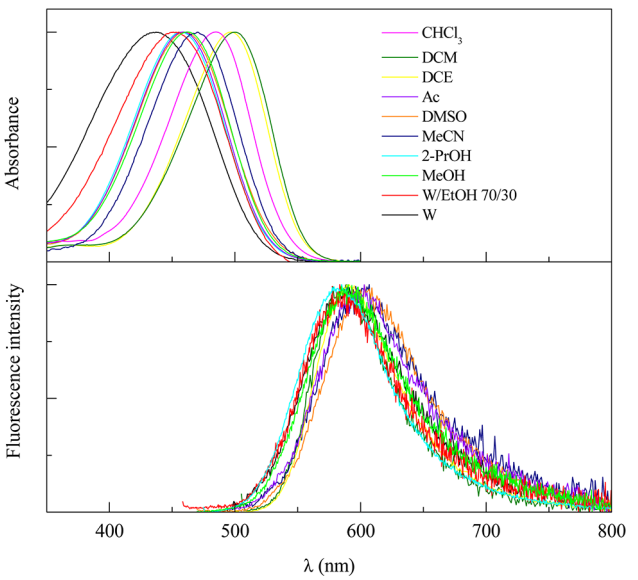

Figure 2. Normalized absorption and emission spectra of **1** in solvents of different polarity.

irradiation and further after relaxation to the TICT states giving rise to a highly Stokes-shifted fluorescence (strong positive fluosolvatochromism).

High absorption coefficients were measured in nonpolar solvents (39700 and 40900 M^{-1} cm^{-1} in $CHCl_3$ and DCM, respectively) while a much lower value was found in W (25700 M^{-1} cm^{-1}), probably due to the increased CT character in polar solvents (see section 3.5).

An analysis of the full width at half-maximum (fwhm) of the first absorption band ($\Delta\bar{\nu}_{1/2}$) of **1** showed that it gradually increases from 3240 to 6060 cm^{-1} on going from DCM to W (being 5090 in 7/3 W/EtOH mixture and 4080 cm^{-1} in MeOH) . This behavior is typical of a net CT on excitation.[12,50] However, the $\Delta\bar{\nu}_{1/2}$ of the emission band was affected much less by the solvent; it only increased by 500 cm^{-1} on going from DCM to W.

The dual- (or multi-) emission, reported in previous works,[24−28] was not evidenced in the stationary fluorescence spectrum of **1**, probably because of similar energies (LE-S_0 and TICT-S_0) involved in the deactivation, but the presence of at least two emitting states of different nature cannot be excluded and would be in agreement with the strong decrease of the

dx.doi.org/10.1021/jp407342q | J. Phys. Chem. A XXXX, XXX, XXX−XXX

Table 2. Spectral Properties[a] of 2 and 3 in Solvents of Increasing E_T^N Parameters

	2			3		
solvent	λ_{abs}/nm	λ_{em}/nm	$\Delta\nu$/cm^{-1}	λ_{abs}/nm	λ_{em}/nm	$\Delta\nu$/cm^{-1}
$CHCl_3$	390	535	6950	400^{sh}, 457	569	4307
DCM	393	559	7690	400^{sh}, 463	588	4590
DCE	393	553	7362	400^{sh}, 462	590	4696
MeCN	369	555	9082	393^{sh}, 429	585	6216
2-PrOH	378	543	8039	397^{sh}, 444	582	5340
EtOH	375	548	8418	397^{sh}, 440	582	5545
MeOH	371	554	8904	394^{sh}, 434	585	5947
MeOH/Gly(50/50)	369	544	8718	394^{sh}, 436	580	5694
W/EtOH(50/50)	362	539	9071	393^{sh}, 431	581	5990
W	353	546	10014	392^{sh}, 420	586	6745

[a]sh means shoulder.

fluorescence quantum yield and kinetic constant (see below, Table 6) on increasing the solvent polarity that implies also small spectral shifts (not parallel to those observed in absorption).

Table 2 and Figures 3 and 4 show the spectral parameters of **2** and **3** in a limited number of solvents. The trimethoxy-substituted compound **2** absorbed at much shorter wavelengths, almost 100 nm, with respect to the dimethylamino analogue (λ_{max} = 390 and 353 nm; ε_{max} = 23700 and 24800 M^{-1} cm^{-1} in $CHCl_3$ and W, respectively), while in the pyrenyl-derivative **3** the main band shifted by ca. 35 nm to the blue (λ_{max} = 462 nm and ε_{max} = 23800 M^{-1} cm^{-1} in DCE). This result was expected due to the reduced donor ability of the pyrenyl and trimethoxyphenyl moieties (see section 3.2) and the consequent reduced CT character of the transition.

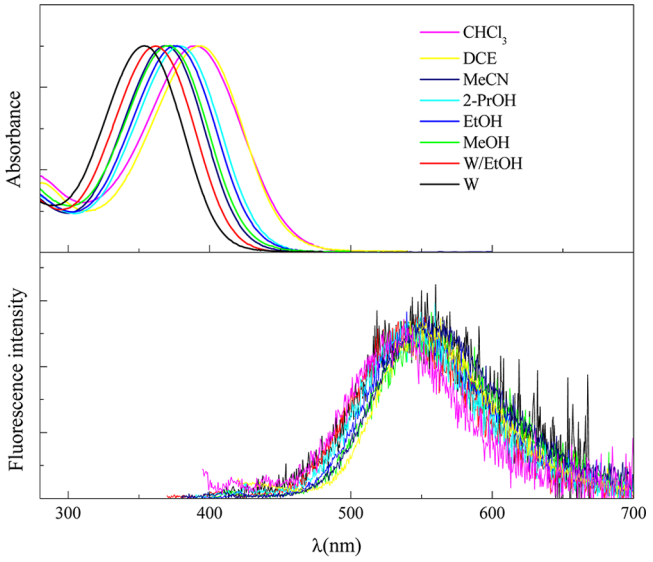

Figure 3. Normalized absorption and emission spectra of **2** in solvents of different polarity.

The absorption spectrum of **3** shifted hypsochromically in polar solvents (λ_{max} = 420 nm and ε_{max} = 21530 M^{-1} cm^{-1} in W) with a shoulder around 395 nm, that was affected little by the solvent. It was assigned to the $\pi\pi^*$ transition that is probably localized at the aromatic group. As found for **1**, the emission spectra of **2** and **3** are quite insensitive to the solvent polarity. Even for them, an absorption shift toward the blue was found in $CHCl_3$ compared with the spectrum in DCM.

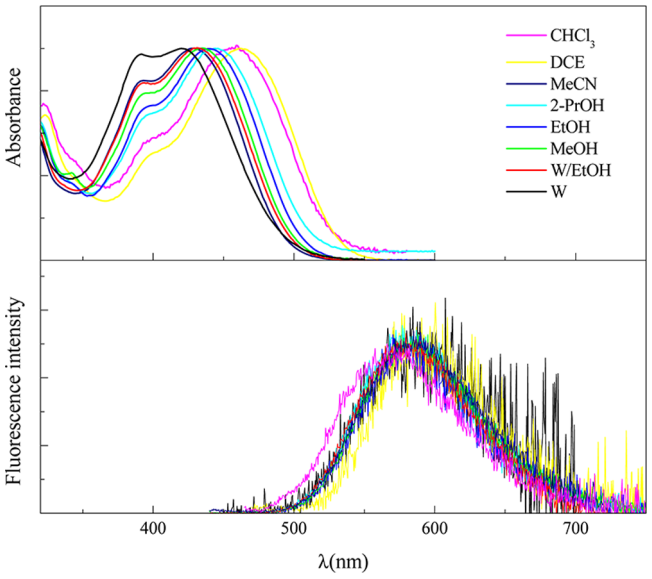

Figure 4. Normalized absorption and emission spectra of **3** in solvents of different polarity.

The absorption and emission spectra of compounds **1**-**3** in a viscous medium (MeOH/Gly, 50/50, v/v) are reported in Figure 1SI (Supporting Information) and compared with those in MeOH (similar solvent polarity). These spectra showed that the solvent viscosity does not affect the spectral shape and position that are mainly determined by the polarity.

Quantum-mechanical calculations by semiempirical methods, reported in Table 1SI for the three compounds, gave spectral results in substantial agreement with the available experimental data (present work and literature data for **1**). The results showed that the first transition (of $\pi\pi^*$ nature and mainly described by HOMO−LUMO configuration) is totally localized in the cation with a partial charge-transfer character (Scheme 1SI).

To further justify the neglect of the counterion we compared the experimental absorption spectrum of compound **1** in MeCN and DCM with those in the same solvents after elution by HPLC (see Figure 2SI) which causes an anion exchange of I^-, replaced (most likely) by Cl^-. The hypsochromic band around 245 nm (characteristic of I^-) is missing after elution, whereas the main bathochromic band is the same before and after elution in both solvents.

3.2. Dipole Moments. The cations of these salts are dipolar A$^+$−π−D systems, where the pyridinium unit A$^+$ is the

dx.doi.org/10.1021/jp407342q | J. Phys. Chem. A XXXX, XXX, XXX−XXX

Table 3. Mulliken Charges and Dipole Moments of 1−3 in DCM Calculated by DFT/B3LYP/3-21G* (S_0) and TD-DFT/B3LYP/3-21G* (S_1) together with the Dihedral Angles θ ($C_9-C_8-C_1-C_2$) and φ ($C_8-C_9-C_{10}-C_{11}$) Showing Rotation of Parts C and A, Respectively

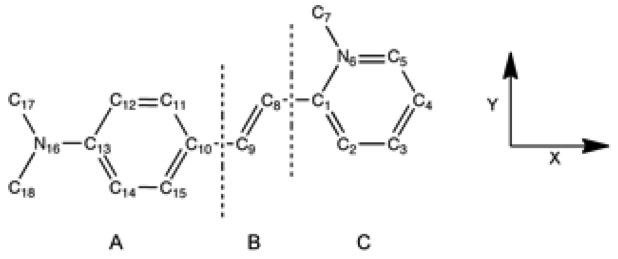

Compound	State	Mulliken charge			μ (D)				θ (deg)	φ (deg)
		A	B	C	μ_X	μ_Y	μ_Z	μ_{Tot}		
1	S_0	0.277	0.058	0.664	6.55	2.06	0.02	6.86	3	0.7
	$S_{1,FC}$	0.499	0.039	0.462	-2.19	2.47	0.02	3.3		
	$S_{1,ICT}$	0.150	0.049	0.802	11.37	1.33	0.9	11.48	81	1
2	S_0	0.128	0.108	0.763	14.59	1.04	0.05	14.62	19	5
	$S_{1,FC}$	0.630	0.008	0.362	-2.87	4.02	3.71	4.94		
	$S_{1,ICT}$	0.075	0.150	0.775	15.69	3.09	2.32	16.16	1	89
3	S_0	0.139	0.105	0.756	18.23	0.23	1.01	18.26	20	19
	$S_{1,FC}$	0.503	0.034	0.463	4.40	0.78	1.26	4.55		
	$S_{1,ICT}$	0.183	0.098	0.719	16.72	0.40	0.57	16.74	5	17

Scheme 2. Calculated Molecular Structure and Dipole Moment Orientation in the Ground State (S_0) and in the FC ($S_{1,v}$) and Relaxed ($S_{1,r}$) Excited Singlet States for 1−3 in DCM

State	1	2	3
S_0	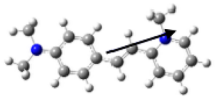	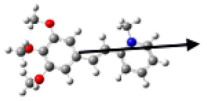	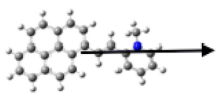
$S_{1,FC}$	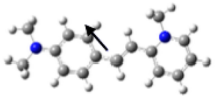	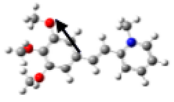	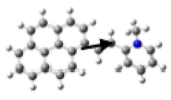
$S_{1,ICT}$	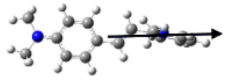	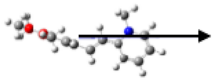	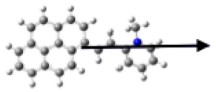

strong acceptor and the dimethylaminophenyl D the strong donor, while the trimethoxyphenyl and pyrenyl groups are D units of moderate donor efficiency, as indicated by their higher halfwave reduction potential (+0.81, +1.42 and +1.16 V vs SCE for **1**, **2** and **3**, respectively).[51] Obviously the dipole moment for an ion is undefined since it depends on the choice of the

dx.doi.org/10.1021/jp407342q | J. Phys. Chem. A XXXX, XXX, XXX−XXX

Scheme 3. Conformational Equilibrium of Cation 1

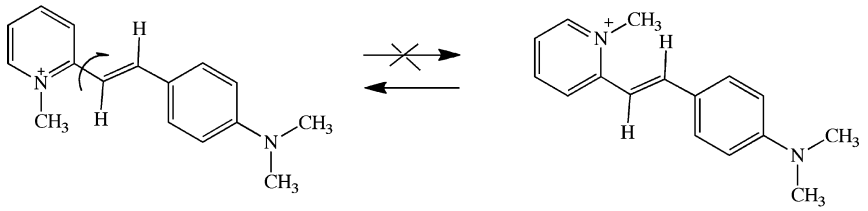

1A 1B

coordinate origin. It is usually convenient to setup a "working definition" based on the center of gravity of the system.[52] Considering that the ICT involving the π-system of the monochromophoric cation is the largely prevailing electronic effect for these salts, one can compare the charge transferred from the D to the A unit upon excitation[51,52] neglecting the counterion.[44] Thus, the dipole moment of the cation can be defined just like that of conventional polar molecules.[43,44] The dipole moments of Table 3 were computed for the ground (S_0) and excited FC ($S_{1,FC}$) states and for the relaxed ICT (or TICT) state formed after completion of the charge movement in the excited state ($S_{1,ICT}$). Table 3 reports also the charge densities calculated for the three moieties of the cation, namely the donor (part A), ethene bridge (part B) and methylpyridinium (part C) groups, as shown in Table 3 for **1**. Calculated molecular structure and dipole moment orientation in S_0, $S_{1,v}$ and $S_{1,ICT}$ states for **1**−**3** in DCM are reported in Scheme 2. Further computational results for **1** in DCM are shown in Table 2SI and Scheme 2SI.

Relatively high values (μ_{S_0} = 6.9, 14.6, and 17.7 D in DCM for **1**, **2** and **3**, respectively, see Table 3) were found for the dipole moment of the most stable ground state conformer (section 3.3) due to the positive charge largely localized on the pyridinium group (see the Mulliken charges in Table 3).

As shown by the MOs in Scheme 1SI and the charge densities in Table 3 the CT character of the transition under light absorption leads to an electron transfer toward the pyridinium group, which reduces the polar character of the FC excited state (μ_{FC} = 3.3, 4.9, and 4.5 D in DCM for **1**, **2**, and **3**, respectively). These results are similar to those reported for the *para*-isomer of **1**[53] and analogous compounds.[54]

The dipole moment component along the principal molecular axis (μ_x, Table 3) changes direction upon excitation only in the case of **1** and **2**, but the total dipole moment (μ_{Tot}, last column of Table 3) of the $S_{1,FC}$ state is reduced for all the three compounds. The relaxed conformation of the $S_{1,ICT}$ state has a twisted geometry in the case of **1** and **2** (the twisting concerning the rotation of methylpiridinium and trimethoxyphenyl groups, respectively) whereas the pyrenyl-derivative retains a planar configuration. The μ_{Tot} of the relaxed S_1 increases and returns to the same direction of the ground state (Table 3) pointing to a relaxation that involves a back charge transfer from C to A moieties. In fact the positive Mulliken charge of the C moiety decreases on excitation and increases again during the relaxation process toward the optimized geometry of S_1.

It should be recalled that while in the nonionic compounds a charge separation is needed for the formation of the $D^+-\pi-A^-$ structure in the perpendicular TICT conformation, in the ionic ones a charge shift, favored in polar solvents, is sufficient.[24,55] In the present case the planar and moderately polar state produced by absorption undergoes a back charge migration and a complete charge shift can be induced by polar solvents, particularly for **1** and **2** where twisting around single bonds favors the localization of the positive charge on the methylpiridinium moiety (C in Table 3) again. This polar TICT state is characterized by a high rate of formation as well as by a quick decay (internal conversion, IC) to the ground state.[43,55,56] This explains why fluosolvatochromism is rarely observed in ionic species where the TICT formation manifests itself through fluorescence quenching. Interestingly, the final increase of the dipole moment leads to a computed μ_{ICT} value slightly higher than μ_{S_0} because the twisting in the excited state assures a better localization of the positive charge with respect to the planar ground state. The particular behavior found for **3**, where twisting does not occur and the dipole moment does not change direction under excitation, leads to $\mu_{ICT} \cong \mu_{S_0}$ and explains why in this compound other relaxation processes become more competitive, particularly ISC[57] and photoisomerization.

Our interpretation of a final S_1 state with the positive charge again localized at the pyridinium moiety appears in contrast with the information available in the abundant literature on **1**. Direct calculations of the charge localization in the relaxed TICT state are not available in previous works, but it can be argued from the reports of different groups that the TICT formation is considered to imply a localization of the positive charge on the twisted donor.[8,25,27] On the contrary, the present calculations (Mulliken charges, molecular structures and dipole moment orientation) seems to clearly indicate that the positive charge in TICT of **1** is returned to the pyridinum moiety. A similar behavior has been found for the twisted compound **2** and for the planar **3**.

3.3. Conformational Equilibria. In principle, the flexible molecules under investigation could exist in fluid solution at room temperature as an equilibrium mixture of conformations[58,59] that originate from the rotation around the quasi-single bonds between the aryl groups and the double bonds. The formation enthalpy (ΔH_f°) calculated by PM3 method and reported in Table 1SI, gave information on the most stable conformer. Compound **1** exists as an equilibrium between two conformers completely shifted toward **1**A at room temperature (Scheme 3). This is in agreement with a λ_{exc}-independent emission spectrum as expected from the coincidence between absorption and fluorescence excitation spectra (see Figure 3SI for **1** in DCM, as an example).

Indeed, the rotation of the methylpyridinium group around the quasi-single bond with the central bridge leads to a steric interaction between the methyl group and the ethenic hydrogen, which is particularly strong in the **1**B conformer. Similar results were obtained for the conformers of **2** and **3**. Even for them, the computed formation enthalpies indicate that the conformers shown in Scheme 1 (**2**A and **3**B of Table 1SI) are expected to be the prevalent species in our solutions.

dx.doi.org/10.1021/jp407342q | J. Phys. Chem. A XXXX, XXX, XXX−XXX

Table 4. Fluorescence and Trans → Cis Photoisomerization Quantum Yields of 1−3 in Various Solvents

	1		2		3	
solvent	$\phi_F \times 10^2$	$\phi_{t\to c}$	$\phi_F \times 10^2$	$\phi_{t\to c}$	$\phi_F \times 10^2$	$\phi_{t\to c}$
$CHCl_3$	5	0.16	0.1	0.07	1.0	
DCM	14	0.16 (0.09)[a]	1.2	0.03 (0.025)[a]	3.3	0.30 (0.20)[a]
DCE	13		3.2		6.0	
MeCN	0.2	<0.001	1.3	0.14	5.3	0.50
2-PrOH			2.1		6.7	
EtOH	1.0	0.064	2.2	0.22	7.3	0.60
MeOH	0.4		1.5		6.9	
MeOH/Gly 50/50	1.9		3.4		7.2	
W/EtOH			0.6		5.4	
W	0.1	<0.001	0.3	0.054	2.8	0.12

[a]Values in parentheses refer to aerated solutions.

3.4. Fluorescence and Photoisomerization Quantum Yields. The quantum yields of the radiative and reactive deactivation pathways of **1**−**3** in solvents of different E_T^N are reported in Table 4. The ϕ_F values of **1** are rather low in the less-polar solvents and decrease further in polar solvents in agreement with the values reported in alcoholic media.[20,23] A similar, although reduced, trend with the E_T^N parameter was observed for **2**. A particularly strange behavior was observed in $CHCl_3$ where the lowest emission yield was measured, probably due to the cited role of ion-pairs in this solvent.[48] A different trend was found for **3** where the ϕ_F value remained practically unchanged, again with the exception of $CHCl_3$. The ϕ_F values were not influenced by molecular oxygen as expected from the very short lifetimes of the lowest excited singlet states (tens or hundreds of ps, see also section 3.5).

The fluorescence quantum yield increased for **1** and **2** in a more viscous medium (MeOH/Gly in Table 4) but remained unchanged for **3** in agreement with twisted (**1** and **2**) and planar (**3**) conformations calculated for the relaxed S_1 state.

The irradiation of the trans isomer of **1**-**3** produced the cis isomer (detected by HPLC) as the only photoproduct (its absorption spectrum is reported in Figures 4SI-6SI for **1**−**3** compounds). The trans → cis photoisomerization of these compounds occurs by the common diabatic mechanism. This implies twisting around the central double bond toward an energy minimum at the perpendicular configuration in the singlet or triplet manifold, followed by $S_1 \to S_0$ internal conversion (IC) or $T_1 \to S_0$ intersystem crossing (ISC) and relaxation to the ground-state trans and cis isomers in roughly a 1:1 branching ratio.[60] The photoreaction yield ($\phi_{t\to c}$) was negligible in polar solvents but increased substantially in nonpolar solvents for **1** (as reported for the analogous *p*-DASPMI[9]) and in all the solvents examined for **2**. The increase was even greater for **3** but in this case solubility problems limited the number of media investigated. The high reactivity of **3** compared to the photostability of 1-styrylpyrene[61] indicates that the pyridinium group strongly reduces the energy barrier to the twisting around the ethene double bond toward the cis geometry.

In contrast to the case of the emissive deactivation, the photoreaction was efficiently quenched by oxygen for **1** in aerated DCM (see Table 4) pointing to a contribution of ISC followed by isomerization in the triplet manifold. This finding is in agreement with the substantial triplet population found for this compound in DCM.[57] The negligible yield of both emissive/reactive deactivation pathways of **1** in polar solvents differs from the results reported for nonionic stilbenoid compounds where a fluorescence decrease is generally coupled with a favored photoisomerization.[60] This probably reflects the fact that in these push−pull compounds in polar solvents one of the two moieties attached to the ethene bridge (anilino or pyridinium group) undergoes a twisting around the single bond with the bridge toward perpendicularity with the formation of the polar TICT state, which in turn undergoes a fast radiationless IC to the ground state. Such behavior is generally assumed for stilbenoid systems including **1** and is supported by the early observation that the rigid analogues have much higher fluorescence yields.[8,23] Instead, the increase of both processes in low polarity solvents may reflect competitive emission and ISC to the triplet manifold,[57] the latter being followed by diabatic isomerization. The more abundant emissive/reactive decay found for **2** and particularly for **3** even in polar solvents indicates that slower ICT processes are operative.

3.5. Femtosecond Transient Absorption. The transient absorption measurements of compounds **1**−**3** were carried out in various solvents of different polarity upon excitation with laser pulses at 400 nm. Figures 5−7 show a contour plot of the experimental data (panel A) and the main time-resolved absorption spectra and kinetics recorded at significant wavelengths (panel B), together with the species associated spectra (SAS) and kinetic properties of the main components obtained by target analysis (panel C) for **1** in DCM and for **2** and **3** in MeOH. Spectral results extended to several other solvents (shown in Figures 7SI-19SI) and data analysis are summarized in Table 5. In particular, the latter shows the time constant τ of each detected transient together with the wavelengths where positive and negative signals, corresponding to decay and growth, respectively, were obtained. In the last column the assignment of the different transients is reported. Fittings of the transient absorption at meaningful wavelengths for **1**−**3** in MeOH and **1** in DCM in all the investigated ps range and at early times (2 ps) are reported, as an example, in Figure 20SI to show the goodness of our fitting models.

Compound 1. The spectrum of **1** in DCM (Figure 5) shows a negative broad band of stimulated emission, formed just after the laser pulse. This band shifts from <540 to 565 nm and grows during the first 0.8 ps; then it shifts from 565 to 600 nm and decays within 390 ps to form a positive transient absorption (rest in Table 5) detected around 580 nm and assigned to the triplet state on the basis of laser flash photolysis results.[57] The data analysis for **1** in DCM (Table 5) showed that three components are present in addition to rest: one with a short lifetime (S) of 0.70 ps, a second one with a medium decay time (M) of 52 ps and a third one with a longer decay

dx.doi.org/10.1021/jp407342q | J. Phys. Chem. A XXXX, XXX, XXX−XXX

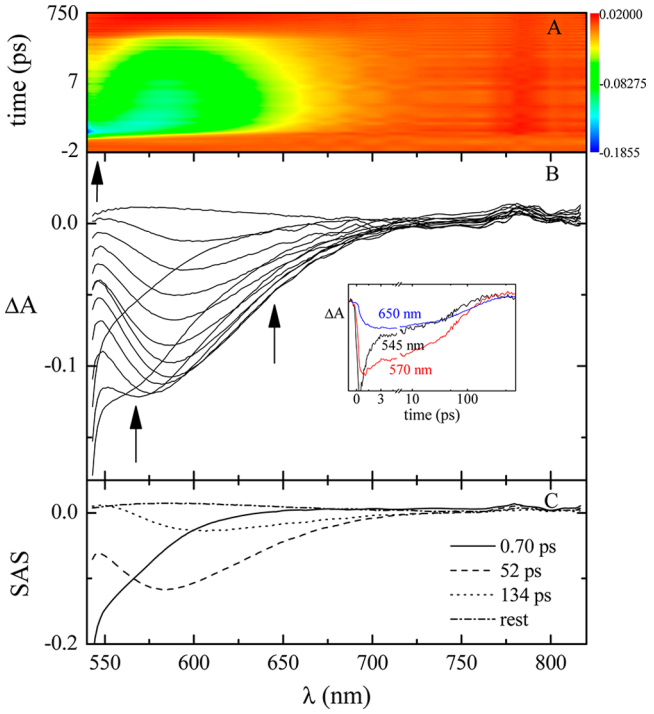

Figure 5. Pump−probe absorption spectroscopy of **1** in DCM (λ_{exc} = 400 nm): (A) contour plot of the experimental data, (B) time-resolved absorption spectra recorded 0.15 (a), 0.45 (b), 0.80(c), 1.2 (d), 2.8 (e), 5.0 (f), 9.2 (g), 17 (h), 38 (i), 56 (j), 97 (k), 170 (l) and 390 (m) ps after the laser pulse (inset: decay kinetics recorded at meaningful wavelengths, with a linear scale for the first picoseconds and log scale for the higher times), and (C) species associated spectra (SAS) calculated by target analysis.

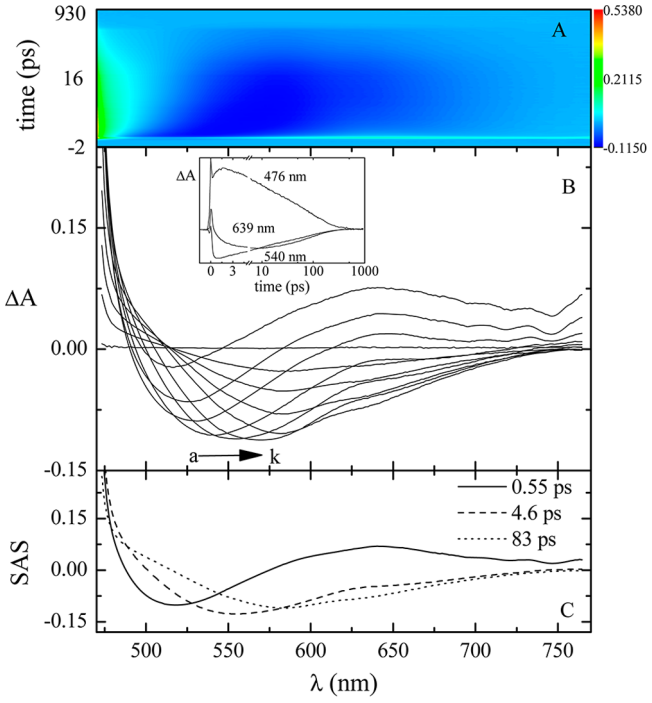

Figure 6. Pump−probe absorption spectroscopy of **2** in MeOH (λ_{exc} = 400 nm): (A) contour plot of the experimental data, (B) time-resolved absorption spectra recorded 0 (a), 0.1 (b), 0.2 (c), 0.6 (d), 1.4 (e), 3.1 (f), 11 (g), 28 (h), 66 (i), 126 (j) and 766 (k) ps after the laser pulse (inset: decay kinetics recorded at meaningful wavelengths, with a linear + log scale), and (C) species associated spectra (SAS) calculated by target analysis.

time (L) of 134 ps. Spectral shapes associated with each component (Figure 5, panel C) were obtained: the transients S, M and L show bands of negative signal centered at <540, 585, and 605 nm, respectively, the two latter in the region of the steady state fluorescence emission spectrum (where the different components are probably buried within the apparently single emission band).[24]

Similar behaviors with different time constants and analogous spectral shapes were found for **1** in other solvents of different polarity (see Figures 7SI-11SI and Table 5). The data analysis in polar solvents reveals three components, generally of shorter time constants if compared with those in less-polar solvents, and the disappearance of the transient rest, in agreement with strong decrease of the triplet yield observed in MeCN by ns measurements.[57] Only two components characterized by the shortest lifetimes (0.7 and 4.4 ps) were detected in the most polar W (see Figure 11SI). Moreover, in polar solvents the transient L showed a spectral shape also characterized by an absorption band at wavelengths around 535 nm (see Figures 7SI and 9SI-11SI). This was not observed in $CHCl_3$, DCM and DCE because of the presence of the red-shifted ground state absorption.

In general, our results are in reasonable/good agreement with those of previous studies in $CHCl_3$ (34 and 79 ps),[27] W (6 ps)[27] and EtOH (4 and 62 ps;[27] ~1, ~6, and 40 ps[28]) even if in some cases the literature data do not include the S transient, due to insufficient resolution time of the equipment.

In agreement with previous results,[23−30] the solvent relaxation is accompanied by a progressive red shift of the stimulated emission band during the first ps after laser excitation indicating that intramolecular processes and solvent relaxation may occur simultaneously[25,62] and that the ICT trajectory is controlled (probably induced) by the solvation process on a ps time scale.

Molecular dynamics calculations on the fastest decays have shown that the solvent response function can be bimodal containing a very fast (inertial motion) component and a red-shifted, much slower (diffusive) component.[63] These should correspond to our S lifetimes (inertial solvation, $Solv_i$, in all solvents) and M lifetimes (diffusive solvation, $Solv_d$, in polar solvents), reflecting the different stages of solvation of the solute.

The role of a biphasic vibrational cooling (VC) process in a few hundreds of fs (solute−solvent energy transfer) and in a few ps (solvent−solvent transfer), as recently reported for two UV dyes (2,5-diphenyloxazole and *p*-terphenyl),[64] can offer an alternative explanation.[65] The latter could be operative due to the significant vibrational excess energy at λ_{exc} = 400 nm. For this reason, the option VC was introduced for the shortest transients observed in all solvents (see last column of Table 5).

The planar and moderately polar LE state described in the literature (evidenced in our ultrafast measurements only in less polar solvents for **1** and **2** and in all solvents for **3**) can be considered to lie in a minimum of the potential energy surfaces with similar geometry and dipole moment of the FC state but vibrationally relaxed. The observation that the solvent dependent dynamics is similar for the three compounds investigated (see below) and is also quite similar for the bridged and unbridged *o*-DASPMI and analogous ionic styryl dyes,[28,63] supports the conclusion that in polar solvents the shortest living S transient, measured at short wavelength, is related to inertial

dx.doi.org/10.1021/jp407342q | J. Phys. Chem. A XXXX, XXX, XXX−XXX

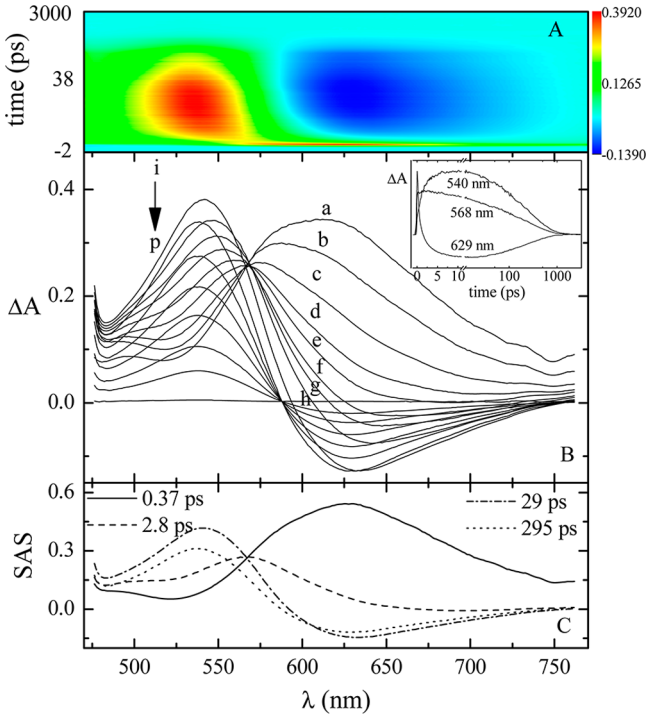

Figure 7. Pump−probe absorption spectroscopy of **3** in MeOH (λ_{exc} = 400 nm): (A) contour plot of the experimental data, (B) time-resolved absorption spectra recorded 0.1 (a), 0.2 (b), 0.4 (c), 0.7 (d), 1.0 (e), 1.5 (f), 1.9 (g), 2.9 (h), 7.8 (i), 34 (j), 78 (k), 128 (l), 214 (m), 354 (n), 534 (o) and 1884 (p) ps after the laser pulse (inset: decay kinetics recorded at meaningful wavelengths, with a linear + log scale), and (C) species associated spectra (SAS) calculated by target analysis.

solvation, while the intermediate lifetime of M is due to diffusive solvation. In fact, the lifetimes of our S/M transients in the polar media (e.g., 0.3/1.2 ps in Ac, 0.19/0.75 in MeCN and 0.22/2.9 in MeOH) are in good agreement with those reported for the polar dynamics of Coumarin 153 (0.187/1.09 ps in Ac, 0.089/0.63 in MeCN and 0.28/3.2 in MeOH).[63] The decay in these solvents is characterized by very small, if any, fluorescence and ISC[57] yields and shorter τ_L values, which reflect the increased efficiency of the return to the ground state by IC. In fact, the presence of TICT states is evidenced by the net fluorescence quenching.

Generally the τ_L values were found to decrease as the solvent polarity increased (from 134 ps in DCM to 4.4 ps in W). This trend becomes clearer if the lifetimes in solvents of the same nature are compared, e.g. in the nonprotic Ac (28 ps) and MeCN (19 ps) and in the protic ones, alcohols and water (94 ps in PrOH, 52 in EtOH, 24 in MeOH, and 4.4 in W). However, in nonpolar media the shift of the positive charge toward a complete ICT is unfavored and the diffusive solvent orientation becomes faster in comparison. In $CHCl_3$ and DCM, the lifetime of the M transient is much longer than the time constants reported for solvation dynamics (26 and 52 ps in our measurements, to be compared with 4.15 and 1.02 ps reported for diffusive solvation in the literature,[63] which are found to be in good agreement with the lifetimes of 2.0 and 0.7 ps obtained for the S transient in $CHCl_3$ and DCM, respectively). In our opinion, this result could be the evidence that in these solvents the M lifetime reflects the rate of the LE → ICT process which is slower and thus becomes the rate controlling step. This finding can explain the higher fluorescence (greater contribution from LE) and/or ISC[57] yields found in these solvents.

Compounds 2 and 3. Analogous studies were carried out for compounds **2** and **3**. The results of SVD and global analysis are also reported in Table 5.

The behavior of the trimethoxy analogue **2** (Figure 6 and Figures 12SI-15SI) is rather similar to that of **1** showing a stimulated emission band red shifting with time. The transient absorption band is out of the investigated spectral range (below 470 nm) in analogy with the hypsochromically shifted absorption observed for the ground state of **2** with respect to **1**. The main difference was found in the longer τ_M and τ_L values which decrease less with increasing the medium polarity. On going from PrOH to W, τ_L decreases by a factor of 25 for **1** but only by a factor of 6 for **2**. This behavior is expected considering the diminished donor properties of the trimethoxy substitution of **2**, which leads to a reduced push−pull character of this compound. It can be noted that the longer τ_M value of **2** with respect to **1**, particularly evident in nonprotic and medium-polarity solvents (Ac, DMSO and MeCN) indicates an ICT process that is slower than diffusive solvation as in less-polar solvents.

An interesting behavior was found for **3**, particularly in solvents of medium and high polarity (see Figures 7, 16SI-19SI and Table 5), since four components resulted from the fitting and the ICT efficiency was further reduced according to the computed planar conformation. Figure 7 shows the spectra in MeOH, where the initial absorption band at 620 nm shifts to 540 nm in around 8 ps. This shift is accompanied by the formation of a negative stimulated emission signal around 630 nm. The formed spectrum decays to zero within 1300 ps. The two components with the shortest lifetimes (S and S′) correspond to the inertial and diffusive solvation parameters. The time constants for M and L were generally found to be longer than those obtained for **1** and **2** in the same solvents (for example, the τ_L value is 19, 93, and 310 ps in MeCN for **1**, **2**, and **3**, respectively). This result indicates that the slower ICT for **3**, not accompanied by twisting (see Scheme 2 and Table 3), makes the two processes (ICT and diffusive solvation) separable in polar solvents, thereby strengthening the transient assignments for **1** and **2**. The reduced ICT character of **3** is also reflected by the reduced effect of the solvent polarity on the time constants of the M and L transients that remain of the same order of magnitude (tens and hundreds of ps, respectively) in all the investigated solvents.

Some fs measurements on compounds **1**-**3** in solvents of increasing viscosity and similar dielectric constant (MeOH/glycerol mixtures) were performed and the results are collected in Table 7SI. They showed three components for **1** and **2** and four for **3** (Figures 21SI-23SI) as in the less viscous media (MeOH) but the time constants increased with the solvent viscosity, as expected for solvent-controlled processes, thus supporting the assignment of the fast transients to inertial and diffusive solvation. The time constant of the longer-lived transient of **1** in MeOH/glycerol mixture (50/50) is 4-fold the value measured in MeOH and twice in the case of **2**, while the time constant of **3** remains practically unchanged in agreement with the planar configuration of the latter in the relaxed $S_{1,ICT}$.

The comparison among some competitive deactivation constants of **1**−**3**, derived on the basis of τ_L in four solvents of different polarity and proticity, was particularly informative (Table 6). On going from DCM to W: (i) k_F decreased notably for **1** but remained almost unchanged for the other two

dx.doi.org/10.1021/jp407342q | J. Phys. Chem. A XXXX, XXX, XXX−XXX

Table 5. Spectral and Kinetic Properties of 1−3 in Solvents of Different Polarity Obtained by Ultrafast Time-Resolved Absorption Spectroscopy at λ_{exc} = 400 nm[a]

	1		2		3		
solvent (E_T^N)	λ/nm	τ/ps	λ/nm	τ/ps	λ/nm	τ/ps	transient
$CHCl_3$ (0.259)	<540(−)	2.0	505(−), 650 (+)	0.35			Solv/VC
	560(−)	26	535(−)	22			^{1}LE*
	590(−)	79	575(−)	44			^{1}ICT*
	570(+)	rest	<480(+)	rest			T_1
DCM (0.309)	<540(−)	0.70	520(−), 635(+)	0.68	590(+)	1.3	Solv/VC
	585(−)	52	555(−)	10	550(+), 640(−)	34	^{1}LE*
	550(+), 605(−)	134	575(−)	172	545(+), 630(−)	424	^{1}ICT*
	580(+)	rest					T_1
DCE (0.327)	<540(−)	0.96	625(+)	0.17	broad	0.1	$Solv_i$ /VC
	590(−)	4.2	530(−), 640(+)	2.3			$Solv_d$/VC
			565(−)	15	550(+)	18	^{1}LE*
	605(−)	177	575(−)	150	540(+), 615(−)	160	^{1}ICT*
	575(+)	rest					T_1
Ac (0.355)	570(−)	0.30	540(−)	0.64	570(+)	0.58	$Solv_i$/VC
	525(+), 605(−)	1.2					$Solv_d$/VC
			580(−)	5.1	545(+), 640(−)	46	^{1}LE*
	540(+), 630(−)	28	585(−)	101	540(+), 630(−)	360	^{1}ICT*
DMSO (0.441)	525(−), 600(+)	0.20	525(−), 590(+)	1.4	585(+)	0.45	$Solv_i$/VC
	585(−)	3.1			575(+)	3.1	$Solv_d$/VC
			560(−)	6.0	550(+), 650(−)	45	^{1}LE*
	540(+), 625(−)	45	585(−)	160	545(+), 635(−)	473	^{1}ICT*
MeCN (0.472)	590(+)	0.19	540(−)	0.33	635(+)	0.15	$Solv_i$/VC
	590(−)	0.75			550(+), 650(−)	0.84	$Solv_d$/VC
			580(−)	3.2	540(+), 640(−)	32	^{1}LE*
	535(+), 625(−)	19	585(−)	93	535(+), 625(−)	310	^{1}ICT*
PrOH (0.546)	535(−)	1.6	505(−), 645(+)	0.93	650(+)	<0.1	$Solv_i$/VC
	575(−)	18	530 (−)	16	600(+)	10	$Solv_d$/VC
					550(+), 635(−)	40	^{1}LE*
	535(+), 600(−)	94	560(−)	135	540(+), 620(−)	386	^{1}ICT*
EtOH (0.654)	540(−)	0.78	510(−), 650(+)	0.64	630(+)	0.83	$Solv_i$/VC
	580(−)	10	535(−)	6.8	570(+)	5.2	$Solv_d$/VC
					550(+), 630(−)	30	^{1}LE*
	535(+), 605(−)	52	575(−)	135	540(+), 625(−)	285	^{1}ICT*
MeOH (0.762)	540(−)	0.22	520(−),640(+)	0.55	630(+)	0.37	$Solv_i$/VC
	580(−)	2.9	550(−)	4.6	570(+)	2.8	$Solv_d$/VC
					545(+), 635(−)	29	^{1}LE*
	535(+), 620(−)	24	580(−)	83	535(+), 625(−)	295	^{1}ICT*
W/EtOH (0.827)	550(−)	0.23	510(−), 645(+)	0.34	615(+)	0.74	$Solv_i$/VC
	580(−)	3.4	535(−)	4.8	565(+)	3.2	$Solv_d$/VC
					545(+), 635(−)	25	^{1}LE*
	525(+), 600(−)	36	565(−)	98	535(+), 630(−)	286	^{1}ICT*
W (1)			535(−)	0.24	650(+)	0.1	$Solv_i$/VC
	570(−)	0.70	550(−)	0.91	550(+)	1.1	$Solv_d$/VC
					540(+), 645(−)	20	^{1}LE*
	520(+), 610(−)	4.4	580(−)	25	535(+), 630(−)	275	^{1}ICT*

[a]Spectral properties refer to species associated spectra (SAS) calculated by target analysis. The symbols (+) and (−) stand for positive and negative signals, respectively.

Table 6. Kinetic Constants (10^8 s^{-1}) of Some Deactivation Pathways of the Excited Singlet Manifold

	1			2			3		
solvent	k_F	k_{IC}	$k_{LE\rightarrow CT}$	k_F	k_{IC}	$k_{LE\rightarrow CT}$	k_F	k_{IC}	$k_{LE\rightarrow CT}$
DCM	10	44	190	0.70	54	1000	0.78		294
MeCN	1.0	520	>13000	1.4	76	3130	1.7	–	313
EtOH	2.1	190	>1000	1.6	40	>1500	2.6	–	333
W	2.3	2270	>14000	1.0	355	>11 000	1.0	26	500

dx.doi.org/10.1021/jp407342q | J. Phys. Chem. A XXXX, XXX, XXX−XXX

compounds, its values (on the order of 10^8 s^{-1}) indicating an allowed transition; (ii) k_{IC} increased by almost two and 1 order of magnitude for **1** and **2**, respectively, while it was much smaller for **3** where the reactive process largely prevails; (iii) $k_{LE \rightarrow CT}$ increased strongly for **1** and **2** but only weakly for **3**.

4. CONCLUSIONS

The experimental and theoretical results of the present work allowed the mechanism of the excited state deactivation of the push−pull compounds **1**−**3** to be reasonably explained. The results reported in the literature for the strongest push−pull compound **1** were generally confirmed and some open questions satisfactorily answered.

Computed values of the formation enthalpies showed that the conformational equilibrium in solutions is completely (for **1**) and largely (for **2** and **3**) shifted toward one of the possible conformers. The weak radiative and reactive decays of the most stable conformer of **1** are sizable in little-polar solvents only, less for **2**, and decrease further in more polar solvents. On the contrary, the small fluorescence yield of **3** changes little with the solvents and its high photoisomerization yield indicates that the less ICT character opens the way to competitive reactive decay.

The ultrafast measurements, extended to a large series of solvents, confirmed previous results for **1** regarding the occurrence, during the lifetime of the excited state, of fast ICT toward a twisted conformation accompanied by a strong fluorescence decrease in polar solvents.

A satisfactory description of the charge motion in the excited state was obtained with the help of calculations (improved in this revised version using more reliable computational methods, as suggested by one of the reviewers).

The positive charge, which is mainly localized on the acceptor pyridinium group in the ground state, moves toward the dimethylanilino donor group under excitation reaching in the FC state a distribution extended over the whole molecule, thus explaining the decrease in the dipole moment under excitation and the negative solvatochromism. Fast relaxation of the FC state (possibly involving both vibrational cooling and solvation) forms the LE state with a geometry close to that of S_0, whose further relaxation leads to back transfer of the positive charge to the final TICT state with a μ_{ICT} value similar to μ_{S_0}. We believe that the LE state (stable intermediate observed in fs measurements) is separated from TICT by a small energy barrier only in the case of compound **1** in the less-polar solvents $CHCl_3$ and DCM (for **2** even in more polar solvents, until to MeCN, and for **3** in all solvents) whereas in more polar solvents the FC state directly relaxes giving back charge transfer to TICT.

The comparison with the behavior of the two new analogues **2** and **3** helped the transient assignment and allowed the effect of a reduced efficiency of the donor moiety on the extent and dynamics of the ICT process to be evaluated. For compound **2**, whose emission yield decreases less in W, and the ICT character is less pronounced, a twisting of the trimethoxyphenyl moiety seems to be favored by calculations. For **3**, whose emission remains practically unchanged in the polar solvent, the charge separation is not accompanied by twisting.

The results obtained in the viscous solvent, that are expected to hinder the torsional movements, are in agreement with the formation of a TICT state for **1** and **2** (increase of both the fluorescence yield and time constants) and a planar ICT state in the case of **3** (no effect observed).

In conclusion, the overall results allowed an interesting analysis of the simultaneous role of the solvation and the ICT process on the behavior of the solvent−solute system for compounds with different push−pull properties to be performed, as summarized in Scheme 4.

Scheme 4. Sketch of the Relaxation Dynamics in Two Limiting Cases: (A) CT Controlled (^{1}ICT* is Twisted for 1 and 2 and Planar for 3); (B) Solvent Controlled

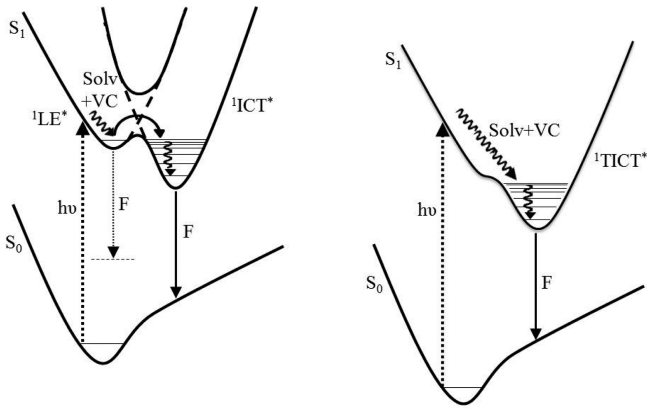

This led us to understand the different behavior of the excited state dynamics in moderately polar solvents for **1** and **2**, where the charge movement is slower than the solvent rearrangement (CT controlled), and in polar solvents, where the situation is inverted (solvent controlled) and a fast barrierless relaxation toward the final ^{1}TICT* state occurs. The dynamics of **3** is CT controlled (A side of Scheme 3) in all the investigated solvents due to the presence of the weaker electron donor pyrene group.

It should be noted that the sensitivity of the spectral behavior of these compounds to the solvent properties and to the light excitation suggests their suitability for use as molecular probes and as elements to elaborate molecular logic units.

■ ASSOCIATED CONTENT

Supporting Information

Additional information on spectrophotometric and fluorimetric measurements, quantum-mechanical calculations, and femtosecond transient absorption in different solvents is available free of charge via the Internet at http://pubs.acs.org.

■ AUTHOR INFORMATION

Corresponding Author

*(A.S.) E-mail: anna.spalletti@unipg.it. Telephone: +390755855575. Fax: +390755855598.

Notes

The authors declare no competing financial interest.

■ ACKNOWLEDGMENTS

The authors thank MIUR (Ministero dell'Università e della Ricerca, Rome, Italy), University of Perugia (PRIN 2010-2011 No. 2010FM738P), for fundings. B.C. also thanks the Regione Umbria (POR FSE 2007-2013, Perugia, Italy) for a fellowship. The authors are grateful to Prof. Eric Vauthey and Dr. Arnulf

Rosspeintner for suggestions useful to the interpretation of the femtosecond measurements. The authors thank also Mr. Danilo Pannacci for his technical assistance in HPLC measurements and Dr. Serena Vannucci and Dr. Marta Moroni for their contributions to the first part of this work during their thesis for the first-level degree in Chemistry.

REFERENCES

(1) Marri, E.; Mazzucato, U.; Fortuna, C. G.; Musumarra, G.; Spalletti, A. Photobehaviour of Some 1-Heteroaryl-2-(1-Methylpyridinium-2-yl)Ethene Iodides (Free and Complexed with DNA). *J. Photochem. Photobiol. A: Chem.* **2006**, *179*, 314−319.

(2) Fortuna, C. G.; Mazzucato, U.; Musumarra, G.; Pannacci, D.; Spalletti, A. Photochemistry and DNA-Affinity of Some Stilbene and Distyrylbenzene Analogues Containing Pyridinium and Imidazolinium Iodides. *J. Photochem. Photobiol. A: Chem.* **2010**, *216*, 66−72.

(3) Mazzoli, A.; Carlotti, B.; Fortuna, C. G.; Spalletti, A. Photobehaviour and DNA Interaction of Styrylquinolinium Salts with Thiophene Substituents. *Photochem. Photobiol. Sci.* **2011**, *10*, 973−979.

(4) Mazzoli, A.; Carlotti, B.; Bonaccorso, C.; Fortuna, C. G.; Mazzucato, U.; Miolo, G.; Spalletti, A. Photochemistry and DNA-Affinity of Some Pyrimidine-Substituted Styryl-Azinium Iodides. *Photochem. Photobiol. Sci.* **2011**, *10*, 1830−1836.

(5) Fortuna, C. G.; Barresi, V.; Bonaccorso, C.; Consiglio, G.; Failla, S.; Trovato-Salinaro, A.; Musumarra, G. Design, Synthesis and In Vitro Antitumour Activity of New Heteroaryl Ethylenes. *Eur. J. Med. Chem.* **2012**, *47*, 221−227 and references therein..

(6) Fortuna, C. G.; Forte, G.; Pittala, V.; Giuffrida, A.; Consiglio, G. Could 2,6-Bis((E)-2-(Furan-2-yl)Vinyl)-1-Methylpyridinium Iodide and Analog Compounds Intercalate DNA? A First Principle Prediction Based on Structural and Electronic Properties. *Comput. Theor. Chem.* **2012**, *985*, 8−13.

(7) Bradamante, S.; Facchetti, A.; Pagani, G. A. Heterocycles as Donor and Acceptor Units in Push-Pull Conjugated Molecules. Part 1. *J. Phys. Org. Chem.* **1997**, *10*, 514−524.

(8) Fromherz, P.; Heilemann, A. Twisted Internal Charge Transfer in (Aminophenyl)Pyridinium. *J. Phys. Chem.* **1992**, *96*, 6864−6866 and references therein..

(9) Görner, H.; Gruen, H. Photophysical Properties of Quaternary Salts of 4-Dialkylamino-4′-Azastilbenes and Their Quinolinium Analogues in Solution: IX. *J. Photochem.* **1985**, *28*, 329−350 and references therein..

(10) Abraham, E.; Oberlé, J.; Jonusauskas, G.; Lapouyade, R.; Rullière, C. Photophysics of 4-Dimethylamino 4′-Cyanostilbene and Model Compounds: Dual Excited States Revealed by Sub-Picosecond Transient Absorption and Kerr Ellipsometry. *Chem. Phys.* **1997**, *214*, 409−423 and references therein..

(11) Pines, D.; Pines, E.; Rettig, W. Dual Fluorescence and Excited-State Structural Relaxations in Donor−Acceptor Stilbenes. *J. Phys. Chem. A* **2003**, *107*, 236−242 and references therein..

(12) Grabowski, Z. R.; Rotkiewicz, K.; Rettig, W. Structural Changes Accompanying Intramolecular Electron Transfer: Focus on Twisted Intramolecular Charge-Transfer States and Structures. *Chem. Rev.* **2003**, *103*, 3899−4031 and references therein..

(13) Carlotti, B.; Spalletti, A.; Šindler-Kulyk, M.; Elisei, F. Ultrafast Photoinduced Intramolecular Charge Transfer in Push-Pull Di-(phenylethenyl) Furan and Benzofuran: Solvent and Molecular Structure Effect. *Phys. Chem. Chem. Phys.* **2011**, *13*, 4519−4528.

(14) Carlotti, B.; Flamini, R.; Marrocchi, A.; Spalletti, A.; Elisei, F. Comprehensive Photophysical Behaviour of Ethynyl-Fluorenes and Ethynyl-Anthracenes Investigated by Fast and Ultrafast Time-Resolved Spectroscopy. *ChemPhysChem* **2012**, *13*, 724−735.

(15) Baraldi, I.; Brancolini, G.; Momicchioli, F.; Ponterini, G.; Vanossi, D. Solvent Influence on Absorption and Fluorescence Spectra of Merocyanine Dyes: A Theoretical and Experimental Study. *Chem. Phys.* **2003**, *288*, 309−325.

(16) Matsui, M.; Kawamura, S.; Shibata, K.; Muramatsu, H. Synthesis and Characterization of Mono-, Bis-, and Trissubstituted Pyridinium and Pyrylium Dyes. *Bull. Chem. Soc. Jpn.* **1992**, *65*, 71−74.

(17) AZ Al-Ansari, I. Interaction of Solvent with the Ground and Excited State of 2- and 4-[4-(Dimethylamino)Styryl]-1-Alkylpyridinium Iodides: an Absorption and Fluorescence Study. *Bull. Soc. Chim. Fr.* **1997**, *134*, 593−599.

(18) Gawinecki, R.; Trzebiatowska, K. The Effect of the Amino Group on the Spectral Properties of Substituted Styrylpyridinium Salts. *Dyes Pigm.* **2000**, *45*, 103−107.

(19) Mishra, A.; Behera, R. K.; Behera, P. K.; Mishra, B. K.; Becera, G. B. Cyanines During the 1990s: A Review. *Chem. Rev.* **2000**, *100*, 1973−2011.

(20) Wang, H.; Helgeson, R.; Ma, B.; Wudl, F. Synthesis and Optical Properties of Cross-Conjugated Bis(Dimethylaminophenyl)-Pyridylvinylene Derivatives. *J. Org. Chem.* **2000**, *65*, 5862−5867.

(21) Huang, Y.; Cheng, T.; Li, F.; Luo, C.; Huang, C.-H.; Cai, Z.; Zeng, X.; Zhou, J. Photophysical Studies on the Mono- and Dichromophoric Hemicyanine Dyes II. Solvent Effects and Dynamic Fluorescence Spectra Study in Chloroform and LB Films. *J. Phys. Chem. B* **2002**, *106*, 10031−10040.

(22) Sahoo, D.; Chakravorti, S. Dye-Surfactant Interaction: Modulation of Photophysics of an Ionic Styryl Dye. *Photochem. Photobiol.* **2009**, *85*, 1103−1109 and references therein..

(23) Strehmel, B.; Rettig, W. Photophysical Properties of Fluorescence Probes I: Dialkylamino Stilbazolium Dyes. *J. Biomed. Opt.* **1996**, *1*, 98−109.

(24) Strehmel, B.; Seifert, H.; Rettig, W. Photophysical Properties of Fluorescence Probes. 2. A Model of Multiple Fluorescence for Stilbazolium Dyes Studied by Global Analysis and Quantum Chemical Calculations. *J. Phys. Chem. B* **1997**, *101*, 2232−2243.

(25) Bingemann, D.; Ernsting, N. P. Femtosecond Solvation Dynamics Determining the Band Shape of Stimulated Emission from a Polar Styryl Dye. *J. Chem. Phys.* **1995**, *102*, 2691−2700.

(26) Jonkman, A. M.; Meulen, P. v.d.; Zhang, H.; Glasbeek, M. Subpicosecond Solvation Relaxation of DASPI in Polar Liquids. *Chem. Phys. Lett.* **1996**, *256*, 21−26.

(27) Ramadass, R.; Bereiter-Hajn, J. Photophysical Properties of DASPMI as Revealed by Spectral Resolved Fluorescence Decays. *J. Phys. Chem. B* **2007**, *111*, 7681−7690.

(28) van der Meer, M. J.; Zhang, H.; Rettig, W.; Glasbeek, M. Femto- and Picosecond Fluorescence Studies of Solvation and Non-Radiative Deactivation of Ionic Styryl Dyes in Liquid Solution. *Chem. Phys. Lett.* **2000**, *320*, 673−680.

(29) Glasbeek, M.; Zhang, H. Femtosecond Studies and Intramolecular Configurational Dynamics of Fluorophores in Liquid Solution. *Chem. Rev.* **2004**, *104*, 1929−1954 and references therein..

(30) Rei, A.; Hungerford, G.; Belsley, M.; Ferreira, M. I. C.; Schellenberg, P. Probing Local Environments by Time-Resolved Stimulated Emission Spectroscopy. *Int. J. Spectrosc.* **2012**, 271435.

(31) Birks, J. B. *Photophysics of Aromatic Molecules*; Wiley-Interscience: London, 1970; p123.

(32) Bartocci, G.; Masetti, F.; Mazzucato, U.; Spalletti, A.; Baraldi, I.; Momicchioli, F. Photophysical and Theoretical Studies of Photoisomerization and Rotamerism of *trans*-Styrylphenanthrene. *J. Phys. Chem.* **1987**, *91*, 4733−4743.

(33) Carlotti, B.; Fuoco, D.; Elisei, F. Fast and Ultrafast Spectroscopic Investigation of Tetracycline Derivatives in Organic and Aqueous Media. *Phys. Chem. Chem. Phys.* **2010**, *12*, 15580−15591.

(34) Del Giacco, T.; Carlotti, B.; Barbafina, A.; De Solis, S.; Elisei, F. Steady-State and Time-Resolved Investigations of a Crown Thioether Conjugated with Methylacridinium and its Complexes with Metal Ions. *Phys. Chem. Chem. Phys.* **2011**, *13*, 2188−2195.

(35) Golub, G. H.; Loan, C. F. V. *Matrix Computations*, 2nd ed. Johns Hopkins University Press: Baltimore, MD, 1989.

(36) Strang, G. *Introduction to linear algebra*; Wellesley-Cambridge Press: Wellesley, MA, 1998.

(37) van Stokkum, I. H. M.; Larsen, D. S.; van Grondelle, R. Global and Target Analysis of Time-Resolved Spectra. *Biochim. Biophys. Acta* **2004**, *1657*, 82.
(38) Copyright © 2009, Snellenburg, J. *Glotaran*; VU University Amsterdam: Amsterdam; http://glotaran.org/.
(39) Frisch, M. J.; Trucks, G. W.; Schlegel, H. B.; Scuseria, G. E.; Robb, M. A.; Cheeseman, J. R.; Scalmani, G.; Barone, V.; Mennucci, B.; Petersson, G. A. et al. *Gaussian 09*, Revision B.01, Gaussian, Inc.: Wallingford, CT, 2010.
(40) Barone, V.; Cossi, M. Quantum Calculation of Molecular Energies and Energy Gradients in Solution by a Conductor Solvent Model. *J. Phys. Chem. A* **1998**, *102*, 1995−2001.
(41) Saunders, V. R.; Freyria-Fava, C.; Dovesi, R.; Salasco, L.; Roetti, C. On the Electrostatic Potential in Crystalline Systems Where the Charge Density is Expanded in Gaussian Functions. *Mol. Phys.* **1992**, *77*, 629−665.
(42) White, J. C.; Hess, A. C. Periodic Hartree-Fock Study of Siliceous Mordenite. *J. Phys. Chem.* **1993**, *97*, 6398−6404.
(43) Rettig, W.; Kharlanov, V.; Maus, M. Excited-State Relaxation Properties of Ionic and Nonionic Donor−Acceptor Biphenyl Derivatives. *Chem. Phys. Lett.* **2000**, *318*, 173−180.
(44) Laage, D.; Thompson, W. H.; Blanchard-Desce, M.; Hines, J. T. Charged Push-Pull Polyenes in Solution: Anomalous Solvatochromism and Nonlinear Optical Properties. *J. Phys. Chem. A* **2003**, *107*, 6032−6046.
(45) Reichardt, C. Solvatochromic Dyes as Solvent Polarity Indicators. *Chem. Rev.* **1994**, *94*, 2319−2358 and references therein..
(46) Görner, H. Charge Transfer Fluorescence of *trans*-Styrylpyridinium Iodides. *J. Photochem. Photobiol. A: Chem.* **2011**, *218*, 199−203.
(47) Bruni, S.; Cariati, E.; Cariati, F.; Porta, F. A.; Quici, S.; Roberto, D. Determination of the Quadratic Hyperpolarizability of *trans*-4-[4-(Dimethylamino)Styryl]Pyridine and 5-Dimethylamino-1,10-Phenanthroline from Solvatochromism of Absorption and Fluorescence Spectra: a Comparison with the Electric-Field-Induced Second-Harmonic Generation Technique. *Spectrochim. Acta* **2001**, *57A*, 1417−1426 and references therein..
(48) Sowmiya, M.; Tiwari, A. K.; Saha, S. K. Study on Intramolecular Charge Transfer Fluorescence Properties of trans-4-[4′-(N,N′-Dimethylamino)Styryl]Pyridine: Effect of Solvent and PH. *J. Photochem. Photobiol., A* **2011**, *218* (1), 76−86.
(49) Tiwari, A. K.; Sarmah, A.; Roy, R. K.; Saha, S. K. Study on Photophysical Properties and Prototropic Equilibria of *trans*-2-[4-(N,N-Dimethylaminostyryl)]Pyridine. *Dyes Pigm.* **2014**, *102*, 114−125.
(50) Marcus, R. A. Relation Between Charge Transfer Absorption and Fluorescence Spectra and the Inverted Region. *J. Phys. Chem.* **1989**, *93*, 3078−3086.
(51) Montalti, M.; Credi, A.; Prodi, L.; Gandolfi, M. T. *Handbook of Photochemistry*; CRC, Taylor & Francis: Boca Raton, FL, 2006; pp 505−510.
(52) Daudel, R.; Lefebvre, R.; Moser, C. *Quantum Chemistry. Methods and Applications*; Interscience Publishers Inc.: New York, 1959, Chapter IX.
(53) Duan, X.-M.; Konami, H.; Okada, S.; Oikawa, H.; Matsuda, H.; Nakanishi, H. Second-Order Hyperpolarizabilities of Stilbazolium Cations Studied by Semiempirical Calculation. *J. Phys. Chem.* **1996**, *100*, 17780−17785.
(54) Zhan, C.-L.; Wang, D.-Y. Nonlinear Dependence of Solvent Polarity Effects on Twisted Intramolecular Charge-Transfer States and Linear Relation for Electronic Spectra in a Stilbazolium-like Dye. *J. Photochem. Photobiol. A: Chem.* **2002**, *147*, 93−101.
(55) Rettig, W. Photoinduced Charge Separation via Twisted Intramolecular Charge Transfer. *Top. Curr. Chem.* **1994**, *169*, 253−299.
(56) Kakitani, T.; Mataga, N. Different Energy Gap Laws for the Three Types of Electron-Transfer Reactions in Polar Solvents. *J. Phys. Chem.* **1986**, *90*, 993−995.
(57) Carlotti, B. et al. To be published.
(58) Mazzucato, U.; Momicchioli, F. Rotational Isomerism in *trans*-1,2-Diarylethylenes. *Chem. Rev.* **1991**, *91*, 1679−1719.
(59) Bartocci, G.; Spalletti, A.; Mazzucato, U. Conformational Aspects in Organic Photochemistry. In *Conformational Analysis of Molecules in Excited States*; Waluk, J., Ed.; Wiley—VCH: New York, 2000; Chapter 5.
(60) Saltiel, J.; Sun, Y.-P. Cis-Trans Isomerization of C═C Double Bonds In *Photochromism: Molecules and Systems*, Dürr, H., Bouas-Laurent, H., Eds.; Elsevier: Amsterdam, 1990; Chapter 3, pp 64−162 and references therein.
(61) Mazzucato, U.; Spalletti, A.; Orlandi, G.; Poggi, G. Effect of the Nature of the Aromatic Groups on the Lowest Excited States of *trans*-1,2-Diarylethylenes. *J. Chem. Soc. Faraday Trans.* **1992**, *88*, 3139−3144.
(62) Kosower, E. M.; Huppert, D. Solvent Motion Controls the Rate of Intramolecular Electron Transfer in Solution. *Chem. Phys. Lett.* **1983**, *96*, 433−435.
(63) Horng, M. L.; Gardecki, J. A.; Papazyan, A.; Maroncelli, M. Subpicosecond Measurements of Polar Solvation Dynamics: Coumarin 153 Revisited. *J. Phys. Chem.* **1995**, *99*, 17311−17337.
(64) Braem, O.; Penfold, T. J.; Cannizzo, A.; Chergui, M. A femtosecond Fluorescence Study of Vibrational Relaxation and Cooling Dynamics of UV Dyes. *Phys. Chem. Chem. Phys.* **2012**, *14*, 3513−3519.
(65) Letrun, R.; Koch, M.; Dekhtyar, M. L.; Kurdyukov, V. V.; Tolmachev, A. I.; Rettig, W.; Vauthey, E. Ultrafast Excited State Dynamics of Donor-Acceptor Biaryls: Comparison between Pyridinium and Pyrilium Phenolates. *J. Phys. Chem. A* **2013**, *117*, 13112−13126.